Sigma J Eng & Nat Sci 38 (4), 2020, 2013-2026

Sigma Journal of Engineering and Natural Sciences
Sigma Mühendislik ve Fen Bilimleri Dergisi

Research Article

DETERMINATION OF THERMAL STRESS AND ELONGATION ON DIFFERENT CERAMIC COATED Ti-6Al-4V ALLOY AT ELEVATED TEMPERATURES BY FINITE ELEMENT METHOD

Berkay ERGENE[1], Çağın BOLAT*[2]

[1]*Pamukkale University, Department of Mechanical Engineering, DENIZLI;* ORCID: 0000-0001-6145-1970
[2]*Istanbul Technical University, Faculty of Mechanical Engineering, Materials and Manufacturing Department, ISTANBUL;* ORCID: 0000-0002-4356-4696

Received: 11.04.2020 Revised: 11.10.2020 Accepted: 04.11.2020

ABSTRACT

Recently, coating applications of hard engineering ceramics on metallic alloys have become notably widespread in order to expand the service life of the critical design components working in though conditions like corrosive/oxidative or erosive/abrasive media. Even though scientific efforts on coating processes and their effects on wear and corrosion performance have been studied for years, there is a lack of investigation about mechanical properties, especially thermo-mechanical features of hard ceramic coated metals. In this paper, on the purpose of determination of the thermal stress distribution, effects of coating materials (Al_2O_3, AlN and TiB_2) and coating thickness (400 µm, 600 µm, and 800 µm) on Von-Mises stress, shear stress and resultant displacement for single and full surface coating models designed on Ti-6Al-4V base material are investigated at 373 K, 573 K and 873 K. The results show that modulus of elasticity and thermal expansion coefficient of coating ceramic materials and base metallic material affect the elongation and stress values observed on designed models significantly. Besides, coating thickness and ambient temperature are also effective on thermal properties. Lastly, it can be pointed out that resultant displacement values on a single-surface coating model are higher than full surface coating model. However, Von-Mises and shear stress values calculated with finite element analysis on single surface coating model is lower than the values read for full-surface coating model.
Keywords: Finite element analysis, Ti-6Al-4V, thermal stress, thermal expansion, ceramic coating.

1. INTRODUCTION

The light metallic alloys working at elevated temperatures and in aggressive environments having potential for corrosion and tribo-corrosion are utilized often in high-tech industrial applications. Only fourteen elements can be defined as light metals because of their density values lower than 4500 kg/m^3. Among these, titanium, aluminum, and magnesium are utilized widely as significant design materials [1]. In today's industrial world, the term of lightness has become extremely crucial due to environmental concerns. Concordantly, the issue of fuel efficiency has been a key point for the automotive and aviation sectors. In this point, it is obvious that structural parts used in the component design must not only have low-density levels but they must also

* Corresponding Author: e-mail: caginbolat@itu.edu.tr, tel: (212) 293 13 00

exhibit sufficient mechanical properties under real service conditions. Compared to other light metals, Ti alloys have a high specific strength, creep resistance, high melting point, corrosion resistance, superior biocompatibility. Hence, from the aerospace industry (landing gears, engine and wing parts) to the health sector (medical implants), many different application areas have been attracted by these versatile materials. [2-4]. Also, titanium displays allotropic transformation at 1115 K (this case is also called ~~as~~ polymorphism) and if the temperature of the metal is below this value, a close-packed hexagonal crystal structure is present, but, above this value, body-centered cubic crystal is seen [1]. Depending on their phase conditions, Ti alloys usually are classified in three different categories namely α, β and α-β alloys, and mechanical/physical behaviors of the selected alloy are affected hugely by the phase structure [5-7].

Apart from their diversified usage in several real applications, Ti alloys are also chosen as base materials for different coating applications in order to obtain long service life against high temperature, wear and corrosive media [8-11]. With the intention of examination of physical, chemical, and mechanical properties of the coated Ti specimens, many coating techniques like nickel plating, ion nitriding, hard ceramic cladding, boronizing, physical vapor deposition (PVD), chemical vapor deposition (CVD) and high velocity-oxygen fuel (HVOF) have been tried to apply by lots of researchers in the technical literature [9, 12-16]. Moreover, in recent times, investigations about fatigue characteristics, high-temperature oxidation, wear and tensile performance of coated Ti alloys have begun to rise in a noteworthy manner [17-19]. If the coating applications of titanium are probed on a sectoral basis, many different examples can be given according to usage purposes and performance requirements. In the automotive industry, Ti-based exhaust pipes, silencers, exhaust valves, and suspension springs are used frequently and these parts are coated with some hard ceramics to block wear/corrosion threat or with the same alloy by means of cold spray method to perform repairing [20]. In analogy to automotive, titanium fuselage parts, propellers, wing elements and engine parts are preferred in aerospace implementations, however, all these elements should be coated against extreme conditions like heat and ice carrying high damage potential [21]. As for biomedical coating efforts, investigations focusing on dental implants, joint prostheses and bone fracture fixation plates have been increasing so as to improve surface performances of titanium based materials [22-23]. Lately, some new innovative coating investigations have also tried on Ti-6Al-4V metal by different research teams. For instance, Yan et al [24] focused on laser cladding Ti-Ni/TiN/TiW+TiS/WS_2 composite coating of Ti-6Al-4V to improve wear performance. Bui et al [25] studied antibacterial coating of Ti-6Al-4V using silver nano-powder mixed electrical discharge machining and they showed that silver content decreased with the increasing depth of coat. In another effort, Prakash et al [26] reported that HA-TiO_2 composite coatings could be tailored on Ti-6Al-4V base material by means of plasma spray deposition for orthopedic applications. Ding et al [27] Ta_2O_5 based coating created on biomedical Ti-6Al-4V alloy through magnetron sputtering and emphasized that formed coating layers were smooth, dense and homogenous. Liu et al [28] examined the effect of heat treatment on microstructure and mechanical properties of TiC/TiB composite coatings on the Ti-6Al-4V. The researchers indicated that microhardness and fracture toughness enhanced with post heat treatment. Almeida et al [29] studied the effect of nitrogen in the properties of diamond-like carbon coating on Ti-6Al-4V substrate and found that incorporation of nitrogen atoms affected the tribology of the coating films in a positive manner. Although a large number of scientific papers can be found comfortably about coating procedures for Ti alloys, and tribological or corrosion performance at dissimilar temperatures of coated Ti alloys, there is a lack of studies conducted on the thermal stress analysis. This circumstance is considerably significant at high temperature due to completely different physical and mechanical properties of titanium base materials and coating materials such as hard oxides, nitrides, borides, different metals or composites. In particular, for providing the design standards without any setback, correct determination of thermal stress difference between Ti alloys and engineering ceramics is very critical.

In this study, our main aim is to figure out thermal properties and thermal stress distributions of hard ceramic coated Ti-6Al-4V alloy by means of the finite element analysis (FEA) at high temperatures. Thanks to detailed FEA, the difference between the base material and coating materials can be interpreted and analyzed in detail. In addition, this paper introduces a comprehensive comparison between different hard coating materials, coating thickness values and coating models to find out their probable effects on the thermal stress features.

2. MATERIALS AND METHOD

2.1. Base and Coating Materials

As a base material, general purpose α-β phase structured Ti-6Al-4V, also known as Ti64, alloy was selected. This grade of titanium dominates the world market in comparison with the other grades by reason of its relatively low density, perfect fracture toughness, good corrosion/oxidation resistance and high biocompatibility. Table 1 shows the chemical composition of Ti-6Al-4V in detail. Besides, this alloy saves weight in designed components and is considerably suitable for jet engines, gas turbines and several airframe parts [31-32]. Therefore, it is also correct to state that the aerospace industry is in the forefront for the total Ti-6Al-4V demand in the market.

Table 1. Chemical composition of Ti-6Al-4V alloy

Element content (%)							
C	Fe	N_2	O_2	Al	V	H_2	Ti
<0.08	<0.25	<0.05	<0.2	5.5-6.76	3.5-4.5	0.01	Balance

As for coating materials, three different hard engineering ceramics like Al_2O_3, AlN and TiB_2 were selected owing to their high hardness, good tribological performance, excellent corrosion resistance and suitability for Ti-6Al-4V coating. If these coating materials are glanced at briefly, Al_2O_3 is a useful oxide ceramic that can create continuous oxide layer and enhances oxidation and thermal shock resistance of titanium alloys [33]. AlN, a covalently-bonded nitride ceramic, does not occur naturally and is synthesized from aluminum and nitrogen elements. Due to its excellent corrosion behavior, high hardness and superior modulus of elasticity, AlN improves corrosion and fretting resistance of Ti-6Al-4V alloy [34]. Titanium diboride (TiB_2) is well known engineering ceramic. On account of its high values of melting point, hardness, surface stability, wear performance and specific density, this extremely hard material is often used in different application areas like armor production and chemical cathode material for reduction of alumina to aluminum [35]. Table 2 given below indicates some major physical properties of both Ti-6Al-4V and selected ceramics respectively.

Table 2. Some physical properties of base and coating materials [35-37]

Property	**Materials**			
	Ti-6Al-4V	Al_2O_3	AlN	TiB_2
Density (kg/m^3)	4430	3970-3980	3260-3300	5430-5700
Melting point (K)	1873	2595	>2748	3396
Specific heat (J/kg.K)	553	880	740	420-540
Thermal conductivity (W/m.K)	7.2	18	140-180	1.7-2.7

2.2. Finite Element Analysis

At the beginning of the FEA work, single-surface coating model (SSCM) (Figure 1a) and full-surface coating model (FSCM) (Figure 1b) were designed in Ansys APDL finite element software program. In these coating models, height and length of the structure were determined as 20 mm and 200 mm respectively. On the other hand, coating thickness was chosen in three different values: 400 µm, 600 µm and 800 µm.

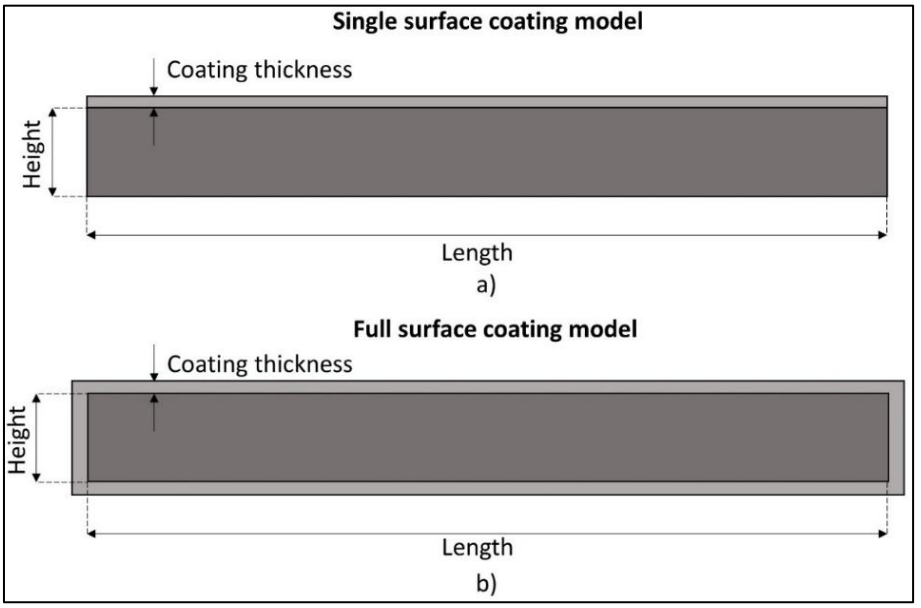

Figure 1. Designed models; SSCM (a) and FSCM (b)

The base material of the designed structure was preferred as Ti-6Al-4V which is an appropriate material to be coated with various engineering materials. As coating ceramics, Al_2O_3, AlN and TiB_2 were appointed. In addition, some mechanical and thermal properties (at temperatures of 373 K, 573 K and 873 K) of these ceramics used in FEA were tabulated in Table 3. In the light of these surface coating models and assigned material properties, totally number of fifty-four 2D-finite element analysis were conducted in structural module of Ansys APDL program.

During FEA, element type of Solid 8 Node 183 was used and Solid 8 Node 183 is a higher order 2-D element with 8 or 6 nodes including quadratic displacement behavior [38]. Additionally, element edge length of 0,2 mm was used to obtain a homogeneous mesh by meshing the coating and base material area finely (Figure 2). Subsequently, all nodes on the line located at left side of the model (indicated with blue color) were constrained to have no displacement along x axis and the centermost node on the same line (indicated with red color) was fixed in all directions as boundary conditions. Lastly, temperature values of 373 K, 573 K and 873 K were applied on all areas like shown in Figure 2. Hence, the effect of temperature on thermal stresses and displacements occurring in SSCM and FSCM with various coating materials was examined in depth.

Table 3. Some mechanical and thermal properties of base and coating materials at specific temperatures [35-37]

Materials	Temperature (K)	Poisson's ratio	Elasticity Modulus (GPa)	Coefficient of Thermal Expansion (10^{-6} 1/K)
Ti-6Al-4V	373	0,31	110	9
	573	0,31	102	9,4
	873	0,31	90	9,7
Al_2O_3	373	0,21	403	6,26
	573	0,21	391	7,31
	873	0,21	370	8,19
AlN	373	0,24	341	4,03
	573	0,24	335	4,84
	873	0.24	326	4,83
TiB_2	373	0,108	562	7,5
	573	0,108	556	7,7
	873	0,108	552	8,04

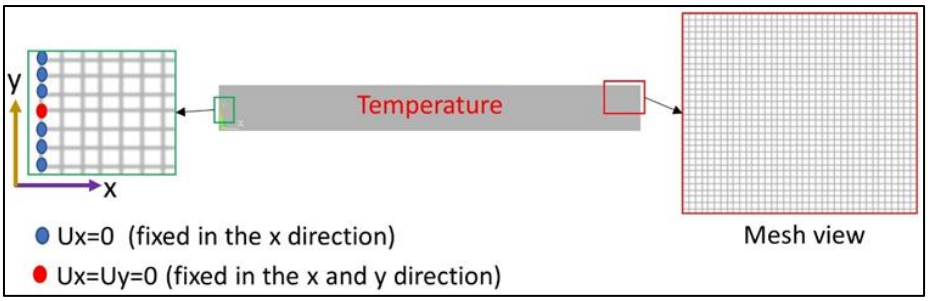

Figure 2. View of applied boundary conditions and mesh on model

3. FEA RESULTS

Firstly, in the FEA, thermal stress distribution on the ceramic coated models was observed. As a consequence of the comparative evaluation, it is very clear from the Figure 3 that TiB_2 coated Ti-6Al-4V samples are exposed to higher stress levels than the others regardless of coating layer thickness, ambient temperature and coating model. This circumstance can be attributed to the high modulus of elasticity values of TiB_2 between 373 K and 873 K. Concordantly, the highest Von Mises stress (σ_{vm}) value of 3729.5 MPa belongs to full-surface TiB_2 coated sample with coating thickness of 800 µm at 873 K even though the lowest σ_{vm} value of 230.7 MPa is measured at 373 K for single-surface AlN coated sample having 800 µm coating thickness. Typically, for all types of coating materials, single-surface coated samples display a downward tendency in the thermal stress values owing to decreasing rigidity and escalating thermal expansion coefficients of ceramics depending upon increasing coating thickness.

Compared to the single-surface coating model, an upward trend is observed for samples having full-surface coating as a result of rising volume fraction of the hard-ceramic coated zones in the sample. Besides, if effects of the ambient temperature are examined, it can be claimed that since the base material of Ti-6Al-4V has better expansion ability, which fluctuates between 9 and 9.7×10^{-6} 1/K, than used hard coating ceramics. Therefore, calculated σ_{vm} values increase for all

models in the same thickness because of the poor elongation ability of titanium (limited by the coating material).

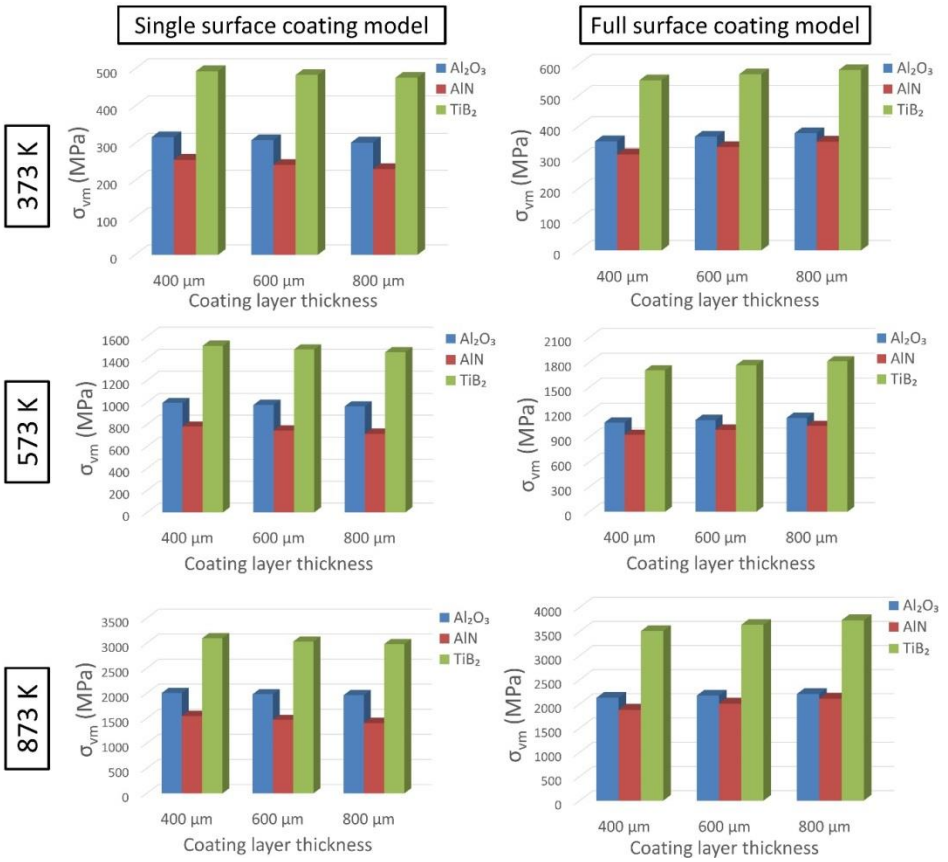

Figure 3. Comparison graphs for σ_{vm} values at various temperatures.

Figure 4 given below shows thermal deformation behavior of simulated models by taking maximum and minimum stress distributions into account. From the simulations, even though single-surface coated samples deform more visibly in the direction of expansion of Ti-6Al-4V (Figure 4a-f), full-surface coated samples remain less deformed due to ceramic coating layers covering the Ti alloy all around (Figure 4g-l). At 373 K, maximum stress concentration accumulates in top right corner on the TiB_2 layer with thickness of 400 µm (Figure 4a), however AlN coated sample having 800 µm coating thickness bears the lowest stress concentration in the same location (Figure 4b). As the temperature rises to 573 K and 873 K respectively, observed σ_{vm} trend continues obviously, and the highest and the lowest σ_{vm} concentration are observed for TiB_2 and AlN coated samples (Figure 4c-f). On the other hand, when the full-surface coated samples are analyzed, it is true to say that stress concentration is localized at bearing point for all temperatures. From Figure 4g, Figure 4i and Figure 4k, at all ambient temperatures, maximum concentration of σ_{vm} values are detected for 800 µm TiB_2 coated samples, at the top left corner of the bearing point. The lowest σ_{vm} concentration on the coating layer is calculated for AlN with coating thickness of 400 µm (Figure 4h, Figure 4j and Figure 4l).

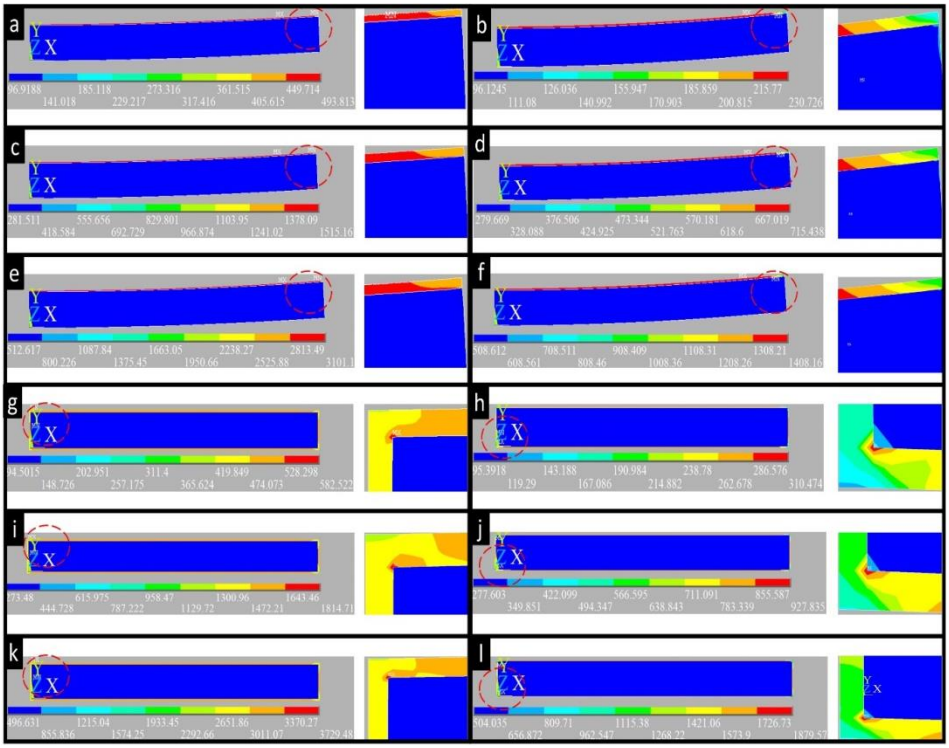

Figure 4. Von-Mises (σ_{vm}) stress distribution on coating models; max. at 373 K for SSCM (TiB_2; 400 µm)(a), min. at 373 K for SSCM (AlN; 800 µm)(b), max. at 573 K for SSCM (TiB_2; 400 µm)(c), min. at 573 K for SSCM (AlN; 800 µm)(d), max. at 873 K for SSCM (TiB_2 ; 400 µm)(e), min. at 873 K for SSCM (AlN; 800 µm)(f), max. at 373 K for FSCM (TiB_2; 800 µm)(g), min. at 373 K for FSCM (AlN; 400 µm)(h), max. at 573 K for FSCM (TiB_2; 800 µm)(i), min. at 573 K for FSCM (AlN; 400 µm)(j), max. at 873 K for FSCM (TiB_2; 800 µm)(k), min. at 873 K for FSCM (AlN; 400 µm)(l)

During the FEA study, shear stress (τ_{xy}) values on the coated samples were recorded and analyzed in detail. Figure 5 depicts a comparison for two types of coating model depending on temperature and coating layer thickness. First of all, contrary to the single layer model, higher τ_{xy} levels are seen on full-surface coated models due to increasing volume fraction of hard/rigid ceramic layer material in the sample. For both coating models, as the ambient temperature goes up, calculated τ_{xy} also rise on account of climbing thermal expansion coefficients of base material and coating ceramics. Similarly, a parallel trend is also recorded for alternating coating layer thicknesses owing to the same reason. When the peak and bottom points are probed, it is correct to express that while the lowest value of 20.3 MPa belongs to single layer 400 µm TiB_2 coated sample in 373 K, the highest value of 865.5 MPa is read for full-surface 800 µm AlN coated sample (873 K). This outcome indicates that mechanical and thermal properties of coating materials at a specific temperature can affect the deformation mechanism sharply. Also, TiB_2 coated sample is subjected to more shear deformation than Al_2O_3 at 573 K and 873 K for both models and at 373 K for FSCM. However, it is observed that TiB_2 loses its superiority over Al_2O_3 at 373 K for SSCM. Regardless of coating model, along with rising ambient temperature and coating thickness, AlN coated samples experience more shear stresses than the others. This

circumstance can be explained with its relatively low thermal coefficient of expansion value in comparison with the Al_2O_3 and TiB_2.

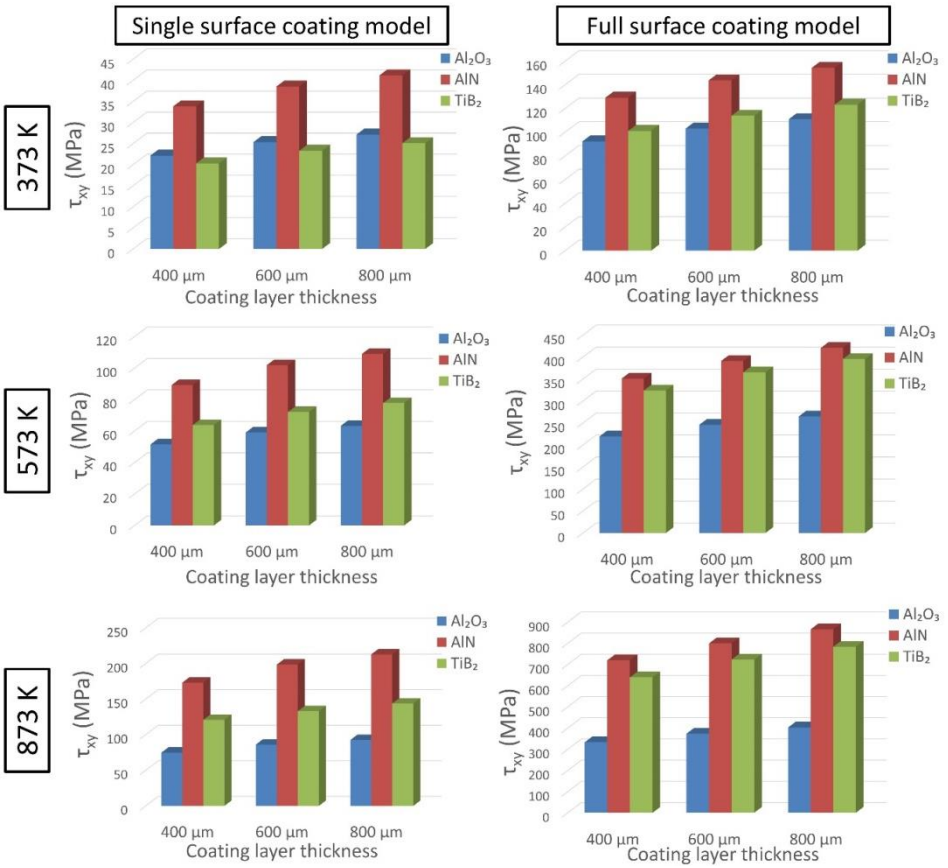

Figure 5. Comparison graphs of ceramic coated models for shear stress (τ_{xy}) values

In order to determine τ_{xy} localizations on the modelled samples, simulation images obtained from FEA are given in Figure 6. Due to high thermal expansion coefficient of Ti-6Al-4V base material, all single-surface coated model samples deform upward direction as estimated before (Figure 6a-f). In terms of shear stress localization, top right sections of the single-surface coated samples are under a noteworthy risk. If the peak τ_{xy} values of 41.1, 109, 212.9 MPa (all measured for AlN coating) are examined, from 373 K (Figure 6a) to 873 K (Figure 6e), an increasing pattern can be seen for both average τ_{xy} and magnitude of the affected zone. In a similar vein, if the lowest τ_{xy} values (all measured for Al_2O_3 coating) are taken into consideration, while 1.3 MPa is found at 373 K (Figure 6b), 2.2 and 3.7 MPa are calculated at 573 K (Fig 6d) and 873 K (Figure 6f) respectively. As for full-surface coated model samples shown between Figure 6g and Figure 6l, the bearing point plays an important role for probable increment in the τ_{xy} concentration since thermal expansion of Ti based alloy is confined by hard ceramic layers. Due to large difference between thermal expansion coefficients of AlN and Ti-6Al-4V alloy, the highest τ_{xy} concentration is detected at 873 K for AlN coated sample with thickness of 800 µm (Figure 6k) although the smallest effect is seen at 373 K for Al_2O_3 coated model with thickness of 400 µm

(Figure 6h). Apart from the stress levels calculated on the models, resultant displacement values are also significant for certain applications by reason of control necessity of dimensional accuracy of the coated parts under different service conditions. In this context, Figure 7 illustrates resultant displacement values of all samples having dissimilar coating models and deformation temperature to compare coating characteristics.

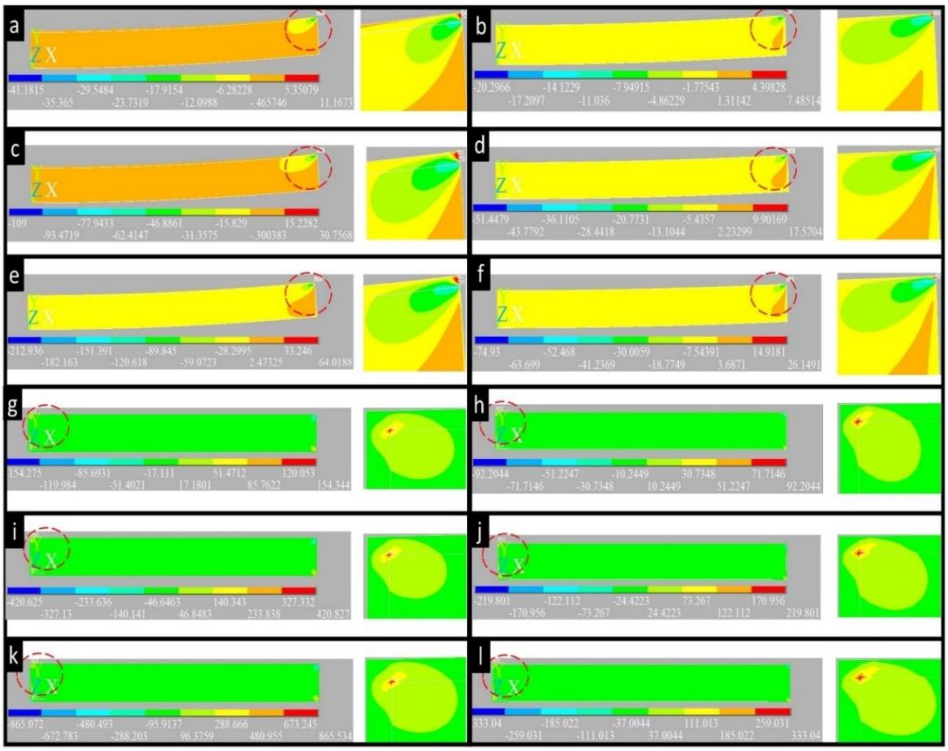

Figure 6. Shear stress (τ_{xy}) distribution on coating models; max. at 373 K for SSCM (AlN; 800 µm)(a), min. at 373 K for SSCM (TiB_2; 400 µm)(b), max. at 573 K for SSCM (AlN; 800 µm)(c), min. at 573 K for SSCM (Al_2O_3; 400 µm)(d), max. at 873 K for SSCM (AlN; 800 µm)(e), min. at 873 K for SSCM (Al_2O_3; 400 µm)(f), max. at 373 K for FSCM (AlN; 800 µm)(g), min. at 373 K for FSCM (Al_2O_3; 400 µm)(h), max. at 573 K for FSCM (AlN; 800 µm)(i), min. at 573 K for FSCM (Al_2O_3; 400 µm)(j), max. at 873 K for FSCM (AlN; 800 µm)(k), min. at 873 K for FSCM (Al_2O_3; 400 µm)(l)

According to FEA results, single-surface coated samples have better displacement ability than their full-surface coated versions at the same temperature values because of the fact that Ti-6Al-4V base material can elongate easily without bottom and right-side confinements. From Figure 7, single layer coated models have the largest elongation capacity than the full-surface models and the highest value is read as 2.69 mm at 873 K for sample having single 800 µm AlN layer. In addition, it can be alleged that as the temperature escalates, elongation capacities of the all ceramic coated models improve due to diminishing rigidity (modulus of elasticity) and rising thermal expansion coefficients of both ceramics and the base alloy. When the full-surface models are analyzed in terms of resultant displacement, compared to AlN and TiB_2, thanks to their moderate elastic modulus and high thermal expansion capacity, Al_2O_3 coated samples exhibit

superior behavior than the others. What's more, since the base metal is covered from all directions by ceramic coating materials, there is a negative relation between coating thickness and displacement ability properties in full-surface coating model samples. This case is observed separately at all temperatures. This situation can be explained with displacement values along y axis. In FSCM, Ti-6Al-4V base material elongates through x axis much more than y axis. Therefore, the effect of elasticity modulus and thermal expansion coefficient values are highly important factors. Moreover, as expected, AlN coated sample exhibits lowest resultant displacement because of its low thermal expansion coefficient. On the other hand, the amount of elongation in the y-axis significantly affects the resultant displacement of the AlN coated sample in the SSCM. In this context, with the help of finite element analysis, a prediction can be made about the thermo-mechanical behavior of the coated samples under real operating conditions.

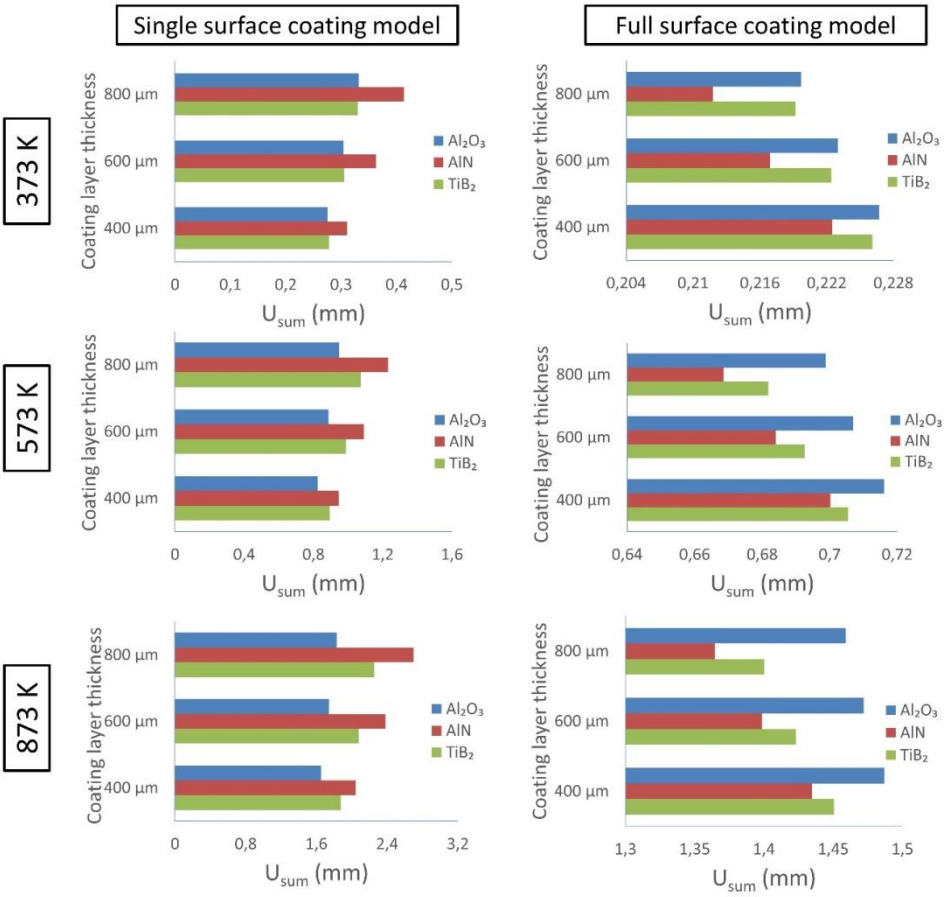

Figure 7. Comparison graphs of ceramic coated models for resultant displacement (U_{sum})

When the simulation details demonstrated in Figure 8 are glanced at carefully, it can be noticed easefully that single-surface coating model samples performs better than the full-surface coating model samples from the point of thermal elongation ability. For single-surface design, at 373 K, maximum and minimum resultant displacement values are 0.27 mm and 0.41 mm for Al_2O_3 and AlN coatings respectively (Figure 8a and Figure 8b). At 573 K (Figure 8c-d) and 873

K (Figure 8e-f), together with the climbing temperature, deformation occurred on top right side of the samples become more apparent. At 573 K, the highest elongation can be found as 1.22 mm (Figure 8c) while this value is 2.69 mm at 873 K (Figure 8e). Nevertheless, if the full surface coating model samples are evaluated, it can be realized that the situation is quite different (Figure 8g-l). All full-surface design samples substantially elongate in the x axis because of confinements stemming from bearing point and frame ceramics. Furthermore, this one-way elongation style is also caused by symmetric structure of coating materials. As for numbers obtained from the FEA, the highest value is determined as 1.48 mm for 400 µm Al_2O_3 coated sample at 873 K (Figure 8k). The lowest displacement is observed as 0.211 mm at 373 K for 800 µm AlN coated sample (Figure 8h). At the intermediate temperature of 573 K, maximum calculated displacement is 0.716 mm for 400 µm Al_2O_3 coating even though minimum value of 0.66 mm belongs to 800 µm AlN coating (Figure 8i-j).

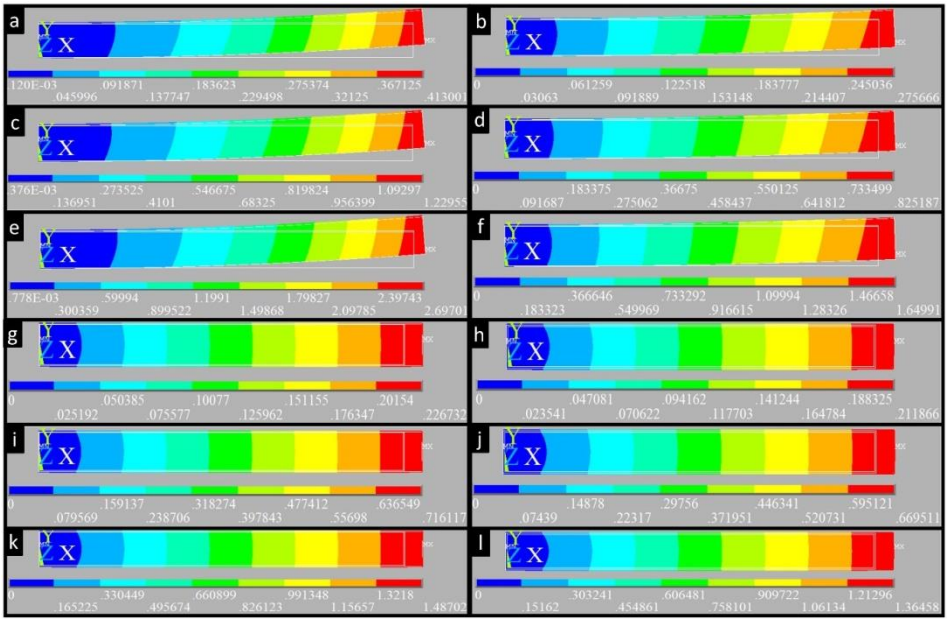

Figure 8. Resultant displacement (U_{sum}) distribution on coating models; max. at 373 K for SSCM (AlN; 800 µm)(a), min. at 373 K for SSCM (Al_2O_3; 400 µm)(b), max. at 573 K for SSCM (AlN; 800 µm)(c), min at 573 K for SSCM (Al_2O_3; 400 µm)(d), max. at 873 K for SSCM (AlN; 800 µm)(e), min. at 873 K for SSCM (Al_2O_3; 400 µm)(f), max. at 373 K for FSCM (Al_2O_3; 400 µm)(g), min. at 373 K for FSCM (AlN; 800 µm)(h), max. at 573 K for FSCM (Al_2O_3; 400 µm)(i), min. at 573 K for FSCM (AlN; 800 µm)(j), max. at 873 K for FSCM (Al_2O_3; 400 µm)(k), min. at 873 K for FSCM (AlN; 800 µm)(l)

In the light of theoretical simulation efforts, it can be claimed that different coating materials, coating thickness and ambient temperatures can change the thermal stress properties of ceramic coated Ti-6Al-4V base material. In addition, since some physical and mechanical properties of the base alloy like thermal conductivity and young modulus alter depending on ambient temperature as some investigators reported [39], single-layer ceramic coated samples are forced an upward motion due to the structure of simulation models while full-surface model samples expand to right side. In this paper, two FEA models were set for three different ceramic coating materials to analyze stress distribution. The FEA study is considerably significant because, sometimes,

experimental results are not enough to figure out thermal stress examination after coating operations on metallic materials [40]. It can be also asserted that although Al_2O_3, AlN and TiB_2 coatings can be formed on Ti-based alloys by means of some different methods such as boronizing, HVOF, and micro arc oxidation, investigations on mechanical properties [13,14,41], especially stress distribution analysis, are difficult tasks for researchers without detailed FEA works. In this point, in this study, following to the FEA study, it was observed that thermal stress and elongation distribution of the coated samples could be predicted. For all ceramic types, the highest stress concentration was detected on the point of support for full-surface model samples whereas the highest shear and Von-Mises stress values were read on the top right side sections of the single-surface samples. According to the FEA results, thermal stress distribution and elongation properties can change depending on dissimilar coating ceramics, so it can be also alleged that alternative coating models, optimum coating thickness and proper part geometry with round corners should be taken into consideration in order to keep corrosion/oxidation resistance and improve the design conditions against the thermal loadings.

4. CONCLUSIONS

As a result of this simulation study focusing on thermal stress and elongation features of hard engineering ceramic coated widely used Ti-6Al-4V alloy, the followings can be listed;

- According to FEM analysis, TiB_2 and AlN coated samples show the highest σ_{vm} and τ_{xy} values for all temperatures respectively.
- AlN coated SSCM samples have superior displacement ability than the others, however, this situation is in favour of Al_2O_3 for FSCM model design.
- Compared to σ_{vm} values, the resultant displacement values and τ_{xy} values calculated for FSCM are obtained considerably different than SSCM due to increasing volume fraction of hard ceramic coating materials.
- σ_{vm} and τ_{xy} localizations largely depend on type of the coating design since both of them localize in top right sides of the parts for SSCM models while the bearing points on the left side are subjected to higher stresses for FSCM models.
- From 373 K to 873 K, FSCM samples possess higher thermal σ_{vm} and τ_{xy} stress levels in comparison with SSCM samples on account of limited displacement of base metal leading to internal stresses.
- For all types of coating materials, SSCM samples display a downward tendency in terms of the thermal stress values owing to decreasing rigidity and escalating thermal expansion coefficients of ceramics depending upon increasing coating thickness. However, an upward trend is observed for samples having FSCM because of rising volume fraction of the hard-ceramic coated zones in the sample.

REFERENCES

[1] Ashby M.F., Jones D.R.H., (2013) Engineering Materials 2 An Introduction to Microstructures and Processing, Fourth edition, *Elsevier Ltd*., USA.

[2] Niinomi M., (1998) Mechanical Properties of Biomedical Titanium Alloys, *Materials Science and Engineering: A*, 243(1–2), 231-236.

[3] Antunes R. A., Salvador C. A.F., Oliveira M. C.L., (2018). Materials Selection of Optimized Titanium Alloys for Aircraft Applications. *Materials Research*, 21(2).

[4] Zhang L.C., Attar H., (2016) Selective Laser Melting of Titanium Alloys and Titanium Matrix Composites for Biomedical Applications: A Review, *Advanced Engineering Materials*, 18(4), 463-475.

[5] Hu D., Pan J., Mao J., Guo X., Ji H., Wang R., (2020) An Anisotropic Mesoscale Model of Fatigue Failure in a Titanium Alloy Containing Duplex Microstructure and Hard α Inclusions, *Materials & Design*, 193.

[6] Correa D. R. N., Kuroda P. A. B., Grandini C. R., Rocha L. A., Oliveira F. G. M., Alves A.C., (2016) Tribocorrosion Behavior of β-type Ti-15Zr-based Alloys, *Materials Letters*, 179, 118-121.

[7] Utama M.I., Park N., Baek E.R., (2019) Microstructure and Mechanical Features of Electron Beam Welded Dissimilar Titanium Alloys: Ti–10V–2Fe–3Al and Ti–6Al–4V, *Metals and Materials International*, 25, 439–448.

[8] Chen X., Liao D., Zhang D., Jiang, X., Zhao P., Xu R., (2020) Effect of Content of Graphene on Corrosion Behavior of Micro Arc Oxidation Coating on Titanium Alloy Drill Pipe, *International Journal of Electrochemical Science*, 15, 710 – 721.

[9] Gao C., Dai L., Meng W., He Z., Wang L., (2017) Electrochemically Promoted Electroless Nickel-Phosphorous Plating on Titanium Substrate, *Applied Surface Science*, 392, 912-919.

[10] Gangatharan K., Selvakumar N., Narayanasamy P., Bhavesh G., (2016) Mechanical Analysis and High Temperature Wear Behaviour of AlCrN/DLC Coated Titanium Alloy, *International Journal of Surface Science and Engineering*, 10.

[11] Oliveira V.M.C.A., Vazquez A.M., Aguiar C., Robin A., Barboza M.J.R., (2016) Nitride Coatings Improve Ti-6Al-4V Alloy Behavior in Creep Tests, *Materials Science and Engineering: A*, 670, 357-368.

[12] Uddin G.M., Jawad M., Ghufran M., (2019) Experimental Investigation of Tribo-mechanical and Chemical Properties of TiN PVD Coating on Titanium Substrate for Biomedical Implants Manufacturing. *International Journal of Advance Manufacturing and Technology*, 102, 1391–1404.

[13] Utu I.D., Marginean G., (2017) Effect of Electron Beam Remelting on the Characteristics of HVOF Sprayed Al_2O_3-TiO_2 Coatings Deposited on Titanium Substrate, *Colloids and Surfaces A: Physicochemical and Engineering Aspects*, 526, 70-75.

[14] Duan Y., Wang X., Liu D., Bao W., Li P., Peng M., (2020) Characteristics, Wear and Corrosion Properties of Borided Pure Titanium by Pack Boriding Near α → β Phase Transition Temperature, *Ceramics International*, 46, 10(B), 16380-16387.

[15] Ramazanov K., Agzamov R., Khusainov Y., Tagirov, A., Nikolaev A., Zolotov, I., (2018) Structural Phase Transformations in Titanium Alloy Ti-6Al-4V at Low-Temperature Ion Nitriding, *28th International Symposium on Discharges and Electrical Insulation in Vacuum, ISDEIV 2018*, Greifswald.

[16] Lin, Y., Lei, Y., Li X., Zhi X., Fu H., (2016) A Study of TiB_2/TiB Gradient Coating by Laser Cladding on Titanium Alloy, *Optics and Lasers in Engineering*, 82, 48-55.

[17] Chou K., Chu, P., Marquis E.A., (2018) Early Oxidation Behavior of Si-coated Titanium, *Corrosion Science*, 140, 297-306.

[18] Ao N., Liu D., Zhang X., Fan K., Shi H., Liu Z., Liu C., (2019) The Effect of Residual Stress and Gradient Nanostructure on the Fretting Fatigue Behavior of Plasma Electrolytic Oxidation Coated Ti–6Al–4V alloy, *Journal of Alloys and Compounds*, 811.

[19] Unal O., Karaoglanli A.C., Ozgurluk Y., Doleker K.M., Maleki E., Varol R. (2019) Wear Behavior of Severe Shot Peened and Thermally Oxidized Commercially Pure Titanium, *Engineering Design Applications*, 92, 461-470.

[20] Soboń D., (2018) Application of Cold Sprayed Coatings in Aviation and Automotive, *Automotive Safety, XI International Science-Technical Conference*, 2018, Casta, Slovakia.

[21] Huang X., Tepylo N., Budinger V.P., Budinger M., Bonaccurso E., Villedieu P., Bennani L., (2019) A Survey of Icephobic Coatings and Their Potential Use in a Hybrid Coating/active Ice Protection System for Aerospace Applications, *Progress in Aerospace Sciences*, 105, 74-97.

[22] Liu B., Shi X., Xiao G., Lu Y., (2017) In-situ Preparation of Scholzite Conversion Coatings on Titanium and Ti-6Al-4V for Biomedical Applications, *Colloids and Surfaces B: Biointerfaces*, 153, 291-299.

[23] Maminskas J., Pilipavicius J., Staisiunas E., Baranovas G., Alksne M., Daugela P., Juodzbalys G., (2020) Novel Yttria-Stabilized Zirconium Oxide and Lithium Disilicate Coatings on Titanium Alloy Substrate for Implant Abutments and Biomedical Application, *Materials*, 13, 2070.

[24] Gao Q., Yan H., Qin Y., Zhang P., Guo J., Chen Z., Yu Z., (2019) Laser Cladding Ti-Ni/TiN/TiW+TiS/WS_2 Self-lubricating Wear Resistant Composite Coating on Ti-6Al-4V Alloy, *Optics & Laser Technology*, 113, 182-191.

[25] Bui V.D., Mwangi J.W., Meinshausen A., Mueller A.J., Bertrand J., Schubert A., (2020) Antibacterial Coating of Ti-6Al-4V Surfaces Using Silver Nano-powder Mixed Electrical Discharge Machining, *Surface and Coatings Technology*, 383.

[26] Singh H., Rana P.K., Singh J., Singh S., Prakash C., Królczyk G., (2020) Plasma Spray Deposition of HA–TiO_2 Composite Coating on Ti–6Al–4V Alloy for Orthopedic Applications, *Advances in Materials Processing.*

[27] Ding Z., Zhou Q., Wang Y., Ding Z., Tang Y., He Q., (2020) Microstructure and Properties of Monolayer, Bilayer and Multilayer Ta_2O_5-based Coatings on Biomedical Ti-6Al-4V Alloy by Magnetron Sputtering, *Ceramics International.*

[28] Chen T., Li W., Liu D., Xiong Y., Zhu X., (2020) Effects of Heat Treatment on Microstructure and Mechanical Properties of TiC/TiB Composite Bioinert Ceramic Coatings in-situ Synthesized by Laser Cladding on Ti6Al4V, *Ceramics International.*

[29] Almeida L.S., Souza A.R.M., Costa L.H., Range E.C., Manfrinato M.D., Rossino L.S., (2020) Effect of Nitrogen in the Properties of Diamond-like Carbon (DLC) Coating on Ti6Al4V Substrate, *Materials Research Express*, 7(6).

[30] Liu S., Shin Y.C., (2019) Additive Manufacturing of Ti-6Al-4V Alloy: A Review, *Materials & Design*, 164.

[31] Singh P., Pungotra H., Kalsi N.S., (2017) On the Characteristics of Titanium Alloys for the Aircraft Applications, *Materials Today Proceedings*, 4(8), 8971-8982.

[32] Uhlmann E., Kersting R., Klein T.B., Cruz M.F., Borille A.V., (2015) Additive Manufacturing of Titanium Alloy for Aircraft Components, *Procedia CIRP*, 35, 55-60.

[33] Jin Q., Xue W., Li X., Zhu Q., Wu X., (2009) Al_2O_3 Coating Fabricated on Titanium by Cathodic Microarc Electrodeposition, *Journal of Alloys and Compounds*, 476(1–2), 356-359.

[34] Goldberg J.R., Gilbert J.L., (2004) The Electrochemical and Mechanical Behavior of Passivated and TiN/AlN-coated CoCrMo and Ti6Al4V Alloys, *Biomaterials*, 25(5), 851-864.

[35] Munro R.G., (2000) Material Properties of Titanium Diboride, *Journal of Research of the National Institute of Standards and Technology*, 105(5), 709–720.

[36] U.S. Titanium Industry Inc.. (2017, August 01). Titanium Alloys - Ti6Al4V Grade 5. AZoM. Retrieved on June 22, 2020 from https://www.azom.com/article.aspx?ArticleID=1547.

[37] Shackelford J.F., Alexander W., (2000) Materials Science and Engineering Handbook, Third edition, *CRC Press*, Florida, USA.

[38] Thompson M.K., Thompson J.M., (2017) ANSYS Mechanical APDL for Finite Element Analysis, *Butterworth-Heinemann*, Oxford, UK.

[39] Veiga C., Dawim J.P., Loureiro A.J.R., (2012) Properties and Applications of Titanium Alloys: A Brief Review, *Reviews on Advance Materials Science*, 32, 133-148.

[40] Sarıkaya O., Çelik E., (2002) Effects of Residual Stress on Thickness and Interlayer of Thermal Barrier Ceramic MgO–ZrO_2 Coatings on Ni and AlSi Substrates Using Finite Element Method, *Materials & Design*, 23(7), 645-650.

[41] Demirbaş Ç., Ayday A., (2018). The influence of Nano-TiO_2 and Nano-Al_2O_3 Particles in Silicate Based Electrolytes on Microstructure and Mechanical Properties of Micro Arc Coated Ti6Al4V Alloy. *Materials Research*, 21(5).